# Impact of remote mutations on metallo-β-lactamase substrate specificity: implications for the evolution of antibiotic resistance

Peter Oelschlaeger[1], Stephen L. Mayo[2], and Juergen Pleiss[3]

[1] Division of Biology, California Institute of Technology, Mail Code 114-96, Pasadena, California 91125

[2] Howard Hughes Medical Institute, Divisions of Biology and Chemistry/Chemical Engineering, California Institute of Technology, Mail Code 114-96, Pasadena, California 91125

[3] Institute of Technical Biochemistry, University of Stuttgart, Allmandring 31, 70569 Stuttgart, Germany

Corresponding author: Juergen Pleiss
phone: (+49) 711-685-3191
fax: (+49) 711-685-3196
email: Juergen.Pleiss@itb.uni-stuttgart.de

**Running title: Substrate specificity of metallo-β-lactamase mutants**

**Abstract**

Metallo-β-lactamases have raised concerns due to their ability to hydrolyze a broad spectrum of β-lactam antibiotics. The G262S point mutation distinguishing the metallo-β-lactamase IMP-1 from IMP-6 has no effect on the hydrolysis of the drugs cephalothin and cefotaxime, but significantly improves catalytic efficiency toward cephaloridine, ceftazidime, benzylpenicillin, ampicillin, and imipenem. This change in specificity occurs even though residue 262 is remote from the active site. We investigated the substrate specificities of five other point mutants resulting from single nucleotide substitutions at positions near residue 262: G262A, G262V, S121G, F218Y and F218I. The results suggest two types of substrates: type I (nitrocefin, cephalothin and cefotaxime), which are converted equally well by IMP-6, IMP-1, and G262A, but even more efficiently by the other mutants, and type II (ceftazidime, benzylpenicillin, ampicillin, and imipenem), which are hydrolyzed much less efficiently by all the mutants, with IMP-1 being the most active. G262V, S121G, F218Y, and F218I improve conversion of type I substrates, whereas G262A and IMP-1 improve conversion of type II substrates, indicating two distinct evolutionary adaptations from IMP-6. Substrate structure may explain the catalytic efficiencies observed. Type I substrates have $R_2$ electron donors, which may stabilize the substrate intermediate in the binding pocket and lead to enhanced activity. In contrast, the absence of these stabilizing interactions with type II substrates may result in poor conversion and increased sensitivity to mutations. This observation may assist future drug design. As the G262A and F218Y mutants confer effective resistance to *Escherichia coli* BL21(DE3) cells (high minimal inhibitory concentrations), they are likely to evolve naturally.

**Key Words:** Metallo-β-lactamase; metalloenzyme; substrate specificity; enzyme evolution; point mutation

β-lactamases hydrolyze β-lactam antibiotics and thereby allow survival of pathogenic bacteria challenged by treatment with these agents. Metallo-β-lactamases (MBLs), also known as class B β-lactamases (Ambler 1980), contain one or two zinc ions and are important components of this antimicrobial defense mechanism. They have become a severe clinical problem due to their broad substrate spectra and potential for horizontal transference (Laraki et al. 1999; Lauretti et al. 1999; Franceschini et al. 2000; Iyobe et al. 2000; Livermore and Woodford 2000).

Class B has been further divided into the three subclasses B1 to B3 based on primary structure, and a general numbering scheme has been suggested (Galleni et al. 2001), which will be used throughout this paper. Subclass B1 is the most intensely investigated, and the structures of four of its members have been solved, either as free enzymes or enzyme-inhibitor complexes (Carfi et al. 1995; Concha et al. 1996; Concha et al. 2000; Garcia-Saez et al. 2003). A detailed catalytic mechanism has been proposed for the hydrolysis of nitrocefin (NIT) by CcrA, a binuclear zinc enzyme from *Bacteroides fragilis* (Wang et al. 1999). A zinc-bound hydroxide acts as a nucleophile and attacks the carbonyl carbon of the β-lactam. Cleavage of the amide bond yields an anionic intermediate, which is stabilized by coordination of the resulting carboxylate to Zn1 and the anionic nitrogen to Zn2. The anionic nitrogen is then protonated to form the product; the protonation is the rate-limiting step in the catalytic cycle. Mutational analyses (Yang et al. 1999; Haruta et al. 2000; Yanchak et al. 2000; Haruta et al. 2001; Materon and Palzkill 2001; Carenbauer et al. 2002; de Seny et al. 2002; Huntley et al. 2003; Hall 2004), NMR studies (Scrofani et al. 1999; Huntley et al. 2000; Huntley et al. 2003), and molecular modeling (Salsbury et al. 2001; Antony et al. 2002; Suarez et al. 2002a; Suarez et al. 2002b; Oelschlaeger et al. 2003a; b) have provided additional information on the structure and dynamics of these binuclear MBLs.

It is not clear whether all substrates form an anionic intermediate as NIT (Fast et al. 2001, Moali et al. 2003). However, based on the following observations, a role of the anionic intermediate for other substrates seems reasonable: (1) benzylpenicillin (PEN) and cephaloridine (LOR) were converted

less efficiently by an engineered mononuclear mutant of the binuclear CcrA ($k_{cat}/K_M$ were 6% and 5% of the wild type $k_{cat}/K_M$s). This decrease in catalytic efficiency is similar to that observed with NIT ($k_{cat}/K_M$ was 3% of the wild type $k_{cat}/K_M$) (Fast et al. 2001). The most likely way that the binuclear enzyme increases $k_{cat}/K_M$ compared to the mononuclear enzyme is by stabilizing the intermediate and thus decreasing the energy barrier of the overall reaction. (2) We were able to model the binuclear imipenemases IMP-1 and IMP-6 in complex with anionic intermediates of the four cephalosporins cephalothin (CEF), cefotaxime (CTX), LOR, and ceftazidime (CAZ) in unconstrained MD simulations (Oelschlaeger et al. 2003b).

Although the evolutionary pathways that led to improved catalytic efficiency toward β-lactam antibiotics among binuclear enzymes are not completely clear, valuable insights can be obtained by comparing the substrate profiles of existing MBL variants, e.g., the imipenemases IMP-1 to IMP-13 (Docquier et al. 2003; Toleman et al. 2003). Thus, Iyobe *et al*. proposed that IMP-3 evolved into the more efficient enzyme IMP-1 via only two mutations (Iyobe et al. 2000). It has also been suggested that merely changing residue 262 of IMP-6 from glycine to serine (IMP-1) stabilizes the anionic intermediate of certain β-lactam substrates bound to the protein, thus enhancing catalysis (Oelschlaeger et al. 2003b).

In addition to naturally occurring variants, artificial mutants can reveal alternate evolutionary pathways to improved catalytic efficiency. Directed evolution methods have been applied to screen for improved serine β-lactamases (Orencia et al. 2001; Voigt et al. 2002) and MBLs (Ponsard et al. 2001; Hall 2004). A method combining computational and experimental screening has been used to generate TEM-1 (class A) variants with increased resistance (Hayes et al. 2002). Focusing on conserved positions in the active site, a mutational study of IMP-1 identified residues essential for efficient zinc binding (Haruta et al. 2000), which was confirmed by crystallography (Concha et al. 2000): Zn1 is coordinated by H116, H118 and H196, and Zn2 is coordinated by D120, C221, and H263. Also, conserved residues were tested for their role in substrate binding: while K224 was found to be important, N233 could be mutated

without significant loss of activity (Haruta et al. 2001). These findings were supported by molecular dynamics simulations (Oelschlaeger et al. 2003a). Materon and Palzkill took these studies further and randomized IMP-1 codons to create a library that allowed all possible amino acid substitutions at all positions in and near the active site (Materon and Palzkill 2001). In addition to confirming essential residues, this approach revealed that many other positions in the active site could tolerate amino acid substitutions; the N233A mutant even converted the investigated substrates more efficiently. Using site-directed mutagenesis, Moali *et al*. recently reported that the importance of a flexible loop covering the active site depends on the nature of the substrate (Moali et al. 2003).

While previous reports focused on the active site, we explored the impact of remote mutations on substrate specificity. The G262S point mutation distinguishing IMP-1 from IMP-6 results in significantly improved catalytic efficiency toward LOR, CAZ, PEN, ampicillin (AMP), and imipenem (IMP) (Iyobe et al. 2000). This change in specificity occurs even though S262 does not ligate the zinc ions and is not in contact with the substrate. Molecular dynamics simulations suggest that this effect occurs indirectly via a domino effect in which the neighboring H263 is rendered less flexible, thus stabilizing the enzyme-substrate intermediate complex for these substrates and enhancing catalytic activity (Oelschlaeger et al. 2003b). In this study, we explore this possibility further by determining the impact of other point mutations in the vicinity of position 262 that are also remote from the active site. We restricted mutants to those that could occur via single nucleotide substitutions, thus focusing on IMP-6 variants that can evolve naturally. All mutants showed altered substrate spectra, some exhibiting significantly improved catalytic efficiencies toward certain substrates. Possible mechanisms for these observations are discussed.

**Results**

*Selection of MBL mutants*

To assess whether other point mutants could have an impact similar to the G262S mutation in IMP-1, three additional residues in this region were selected for mutagenesis: K69 and S121 are both within 6 Å of the S262 Oγ and Zn2; F218 is behind the S262 side chain relative to Zn2 and H263. As with S262, these positions are remote from the active site; they do not coordinate the zinc ions or have direct contact with the substrate. We restricted the amino acid substitutions to those that could be achieved by mutating a single nucleotide; a total of 24 fit this criterion; 12 of these result in an altered charge or a cysteine and were excluded to avoid disturbance of the active site. Multiple molecular dynamics (MD) simulations with different starting conditions were performed on the remaining 12 mutants in complex with the CAZ intermediate to predict their catalytic efficiency as reported (Oelschlaeger et al. 2003b). Five mutants, which obtained the highest stability scores based on the number of simulations with stable enzyme-substrate intermediate complexes (data not shown), indicating relatively high catalytic efficiencies, were chosen for experimental validation: S121G, F218Y, F218I, G262A, and G262V (Fig. 1). The MD study will be published elsewhere.

*Expression and biophysical characterization*

All enzymes were expressed well upon isopropyl-β-*D*-thiogalactopyranoside (IPTG)-induction (~50% of total cell protein as estimated from SDS-PAGE). A fair amount of IMP-6, IMP-1, G262A, and F218Y was found in the soluble fraction, indicating good folding behavior in vivo, whereas G262V and S121G folded less efficiently (Table 1). Due to even less efficient folding, the amount of purified protein obtained for mutant F218I was insufficient to determine its zinc occupation (only 150 nM after purification). Circular dichroism spectra of the purified mutant and wild type enzymes were superimposable and characteristic of proteins containing α-helices and β-sheets (data not shown), indicating that the secondary structures are

comparable and consistent with the αββα fold typical for metallo-β-lactamases (Carfi et al. 1995). Two zinc ions are bound per protein molecule for all enzymes except mutant S121G, which contains three zinc ions (Table 1).

*Kinetic constants*

When purified enzyme at low concentrations was not protected, enzymatic activity decreased after incubation at temperatures between 4 and 37 °C and especially after freezing and thawing (data not shown). In agreement with previous reports (Laraki et al. 1999, Siemann et al. 2002), loss of activity could be avoided by adding bovine serum albumin (BSA) after purification. Activity profiles of the wild-type and mutant enzymes were generated with seven substrates: NIT, CEF, CTX, CAZ, PEN, AMP, and IMP; substrate structures are illustrated in Fig. 2. These are the same substrates that Iyobe *et al.* used (Iyobe et al. 2000), except that NIT was included instead of LOR, which is no longer commercially available. The catalytic efficiencies ($k_{cat}/K_M$s) of the wild type enzymes IMP-1 and IMP-6 are shown in Fig. 3. Separate $k_{cat}$ and $K_M$ values are listed in Table 2. The activity of IMP-1 toward NIT is in excellent agreement with reported data: we obtained a $k_{cat}/K_M$ of 23.8 $s^{-1}\,\mu M^{-1}$, while Materon and Palzkill (Materon and Palzkill 2001) and Siemann et al. (Siemann et al. 2002) reported values of 25.3 and 21.7 $s^{-1}\,\mu M^{-1}$, respectively (Fig. 3A). The catalytic efficiency of IMP-6 toward NIT is similar (28.0 $s^{-1}\,\mu M^{-1}$). The activity profiles for the other substrates are in agreement with those reported by Iyobe et al. (Iyobe et al. 2000): CEF and CTX are hydrolyzed equally by the two wild-type enzymes, whereas IMP-1 is more efficient than IMP-6 for CAZ, PEN, AMP, and IMP (Fig. 3B).

The activities of the wild-type and mutant enzymes toward each of the substrates are compared in Fig. 4 and Table 2. The activity profiles suggest two types of substrates: type I (NIT, CEF, and CTX) and type II (CAZ, PEN, AMP, and IMP). For type I substrates, F218I is always the most efficient enzyme (5- to 10-fold over wild types), followed by G262V, S121G, and F218Y (about 2- to 4-fold over wild types). IMP-6, IMP-1 (G262S), and G262A are all

about the same and are the least efficient. In contrast, for type II substrates, IMP-1 is always the most efficient enzyme, followed by G262A, then IMP-6 or F218Y. Conversion by the other enzymes is less efficient and mutant G262V is almost inactive. In addition, all the enzymes hydrolyze type I substrates more efficiently than type II substrates. $k_{cat}/K_M$s are higher by up to four orders of magnitude; values range from about 3 to 240 $s^{-1}\,\mu M^{-1}$ for type I substrates, and from about 0.01 to 3 $s^{-1}\,\mu M^{-1}$ for type II substrates. Substrate inhibition kinetics (see Materials and methods for details) was observed with NIT for mutants S121G and F218Y (see Table 2). Best fits were obtained by setting the number of unproductively bound substrate molecules to one. The inhibition constants $K_i$ were 146 μM for F218Y and 54 μM for S121G.

*Effect of MBLs on susceptibility in vivo*

In order to test how the measured catalytic efficiencies translate to antibiotic resistance conferred to *E. coli* BL21(DE3) host cells, minimum inhibitory concentrations (MICs) were determined following a recently published method (Hammond et al. 1999) (Table 3). IMP-6, IMP-1, G262A, F218Y, and S121G all confer high resistance levels toward the type I substrates CEF and CTX (at least 64-fold compared to cells lacking MBL expression), whereas G262V and F218I only confer 4- to 16-fold resistance level. NIT could only be applied at low concentrations (up to 128 μg/ml) due to poor solubility. All cells including the control cells grew at these concentrations. For type II substrates, cells expressing IMP-1 exhibit the highest resistance levels, followed by those expressing G262A, IMP-6, F218Y, and S121G. G262V and F218I confer either no or only up to 4-fold increased resistance levels. In general, the increase in resistance levels toward CAZ is very low (at the highest 4-fold) or not detectable.

**Discussion**

*Catalytic efficiencies*

The results of this study confirm our previous observations (Oelschlaeger et al. 2003b) and suggest that there are two types of substrates: type I (NIT, CEF, and CTX), which are hydrolyzed equally by IMP-6 and the G262S mutant IMP-1, and type II (CAZ, PEN, AMP, and IMP), which are hydrolyzed much more efficiently by IMP-1 (Iyobe et al. 2000). The G262A mutant exhibits a similar activity profile as IMP-1. We expected that the G262V mutation would also have no impact on hydrolysis of type I substrates, and that mutations more distant from the active site (S121G, F218Y, and F218I) would be equally ineffective. Surprisingly, these mutants all hydrolyze type I antibiotics much more efficiently than IMP-6, IMP-1, and G262A, in spite of their poor capability to hydrolyze type II substrates. The structural features of the two substrate groups may explain the differences observed as described in the domino effect model (Oelschlaeger et al. 2003b): type I β-lactams (NIT, CEF, and CTX) have an electron donor $R_2$ side chain (Fig. 2) and are stabilized by residues around the binding pocket, especially the N233 backbone amide. Thus, the $R_2$ groups are kept away from H263 and do not interfere with its ability to ligate Zn2 (Concha et al. 2000) and stabilize the substrate-intermediate complex (Wang et al. 1999). On the other hand, type II substrates have axial methyl groups (PEN and AMP) or positively charged $R_2$ side chains (CAZ and IMP) and therefore do not contain stabilizing electron donors. Thus, the side chains of these substrates are more mobile and can interfere with the zinc ligand H263. This may disturb the stability of the complex between Zn2 and its ligands including the anionic nitrogen of the substrate intermediate, which might result in lower stability of the intermediate complex and lower catalytic efficiency. As observed in our previous MD simulations (Oelschlaeger et al. 2003b), instability of the intermediate complex is characterized by the dissociation of the anionic nitrogen from Zn2 but not in dissociation of the other ligands. Thus, the binding of Zn2 to the enzyme is very likely not affected.

*Conversion of type II substrates*

The flexibility of H263 may explain the increasing efficiencies of IMP-6, G262A, and IMP-1 with type II substrates. In IMP-6, H263 is relatively flexible (Oelschlaeger et al. 2003b) since glycine at position 262 provides little support; therefore, type II substrates can move H263 and disrupt its ability to ligate Zn2. However, if we replace glycine 262 with alanine, the methyl side chain improves packing and provides more support for H263, which decreases its flexibility and improves catalytic efficiency. IMP-1 decreases H263's flexibility even further, since S262's hydroxymethyl group not only provides improved packing, but also interacts electrostatically with K69; this interaction positions the neighboring P68's carbonyl oxygen to form a hydrogen bond to H263's Nδ (Oelschlaeger et al. 2003b). However, the larger isopropyl side chain in G262V apparently is too bulky, since this mutant was the least active for type II substrates. Instead of being supported by the valine side chain, H263 may be forced into the binding pocket. H263 could then push on type II substrates, which are not stabilized by the N233 backbone amide, and dislocate them so the substrate's anionic nitrogen cannot bind efficiently to Zn2. The S121G mutant was 2- to 4-fold less active than IMP-6. Replacing a serine with glycine at this position may decrease support of the Zn2 ligands H263 and D120, leading to even greater instability of the enzyme-substrate intermediate complex. The catalytic efficiency of F218Y was comparable to IMP-6, suggesting that the additional hydroxyl group has no effect. The mutant F218I was less active than either IMP-6 or F218Y. The F218I mutation might lead to overpacking under the pressure of type II substrates due to the Cβ-branched isoleucine or indirectly affect Zn2 coordination by C221, which is separated from position 218 by only two glycines.

*Conversion of type I substrates*

Surprisingly, the F218I mutation was the most beneficial for type I substrates. In this case, the substrates are stabilized by the N233 backbone amide and do not push toward H263 and the region beyond it, so that now altered packing or the indirect effect via C221 could result in improved

stability of the enzyme-substrate intermediate complex, and enhanced catalytic activity. Merely adding a hydroxyl group with F218Y leads to less dramatic improvement. The S121G mutation also had a beneficial effect on the hydrolysis of type I substrates. When the $R_2$ side chains do not interact with H263, it is feasible that the increased flexibilities of H263 and D120 conferred by the S121G mutation stabilize the active site by allowing Zn2 to turn and obtain better coordination geometry. G262V also showed improved activity, perhaps by moving H263 into the substrate binding pocket and allowing tighter binding of the substrate intermediate. As observed for the two wild types IMP-6 and IMP-1, the G262A mutant had no effect on hydrolysis of type I substrates. This is not surprising since alanine is structurally intermediate to glycine (IMP-6) and serine (IMP-1).

*Substrate inhibition*

Substrate inhibition kinetics was observed for mutants S121G and F218Y with NIT, but not for any of the other substrates tested. The molecular basis for this phenomenon is not clear and the nature of the inhibiting agent cannot be determined, yet. As good fits were obtained by setting the number of unproductively bound molecules to one, either the β-lactam substrate, the anionic intermediate, or the β-amino acid product could inhibit the enzyme. However, as we do not know that, yet, we refer to this phenomenological observation as substrate inhibition, according to the report of Simm and coworkers (Simm et al. 2001). At this point, it is noteworthy that the S121G mutant binds three zinc ions per molecule, as determined with the PAR assay, while F218Y only binds two zincs. The $K_1$ of mutant S121G is three-fold lower than that of F218Y. The third zinc ion may interact electrostatically with the conjugated Π-electron system of the negatively charged NIT intermediate (Wang et al. 1999; Fast et al. 2001), binding the substrate intermediate more tightly and resulting in substrate inhibition. The fact that none of the other substrates tested have such an extensively conjugated Π-electron system may explain why they did not exhibit substrate inhibition kinetics. CcrA is

another MBL with nearly identical active site residues and geometry as IMP-6 and IMP-1 (Concha et al. 1996). However, in addition to two zinc ions, it has a sodium ion at the position corresponding to IMP-6's K69 Nζ (in CcrA, residue 69 is a serine). CcrA's sodium ion is coordinated by the two backbone carbonyls of N70 and D120 and the D84 carboxylate. IMP-6 has the same potential ligands for a third metal ion: the D84 carboxylate and the backbone carbonyls of H70 and D120 (Concha et al. 2000). However, in IMP-6, the D84 carboxylate is not available, since it interacts with the hydroxyl of S121. Glycine at this position in mutant S121G could allow the D84 carboxylate to coordinate a third zinc ion. The third zinc ion could increase electrostatic interactions with the substrate and explain why this mutant shows substrate inhibition kinetics with NIT while the other mutants do not. The ability of S121G to unproductively bind a substrate intermediate may prove useful in that it could facilitate crystallization and allow determination of the first MBL-substrate intermediate complex structure.

The substrate inhibition observed with F218Y and NIT is more difficult to explain because only two zinc ions were observed for this mutant with the PAR assay. One possibility is that the hydroxyl group of Y218 provides a ligand for a third zinc ion, which could be bound during kinetic measurements. However, the affinity of the third zinc ion may be so low that it dissociates during dialysis against zinc-free buffer and is therefore not observed with the PAR assay.

*In vivo resistance levels*

MICs reflect not only catalytic efficiencies, but also expression levels, folding behavior and accessibility of the enzymes by the substrate within the *E. coli* cells. The well-folding mutants G262A and F218Y (Table 1) confer resistance to type I substrates similar to the wild types, whereas for the less efficiently folding mutants the MICs are slightly (S121G) or significantly (F218I and G262V) lower (Table 3). Note that although F218I folded significantly less efficiently than G262V, it confers a higher resistance level, consistent with the high catalytic efficiencies measured

(Table 2 and Fig. 4). The observation that the MICs with F218Y were not higher than e.g. with IMP-6 as observed for catalytic efficiencies, can be explained by the fact that these catalytic efficiencies are extremely high and other factors such as transport or diffusion of the substrate molecules within the cell may become rate-limiting.

For most of the type II substrates (PEN, AMP, and IMP), the observed MICs can also be explained by the catalytic efficiencies (Table 2 and Fig. 4) and in vivo folding (Table 1). Among the well-folding IMP-6, IMP-1, G262A, and F218Y, IMP-1 always confers the highest resistance, followed by G262A, IMP-6, and F218Y. The lower MICs for the other mutants may be explained by lower catalytic efficiencies (S121G and G262V) and less efficient in vivo folding (F218I). Although generally very low compared to the control cells, resistance levels toward CAZ are also highest with IMP-1, followed by G262A and IMP-6. For the other mutants they cannot be distinguished from the control cells. Iyobe et al. (Iyobe et al. 2000) also did not observe MICs consistent with catalytic efficiencies for CAZ and LOR, a cephalosporin with the identical positively charged $R_2$ side chain as CAZ. Possible explanations for this observation include poor transport of CAZ across the *E. coli* cell membranes and within the cytosol, where the MBLs are expressed.

*Implications for imipenemase evolution and drug design*

The data presented here suggest two different strategies that bacteria might adopt to achieve antibiotic resistance through improved MBL activity. In IMP-6, type II substrates (CAZ, PEN, AMP, and IMP) push toward H263, disturbing its coordination to zinc and decreasing the stability of the enzyme-substrate intermediate complex and the transition state. Catalytic efficiency toward these substrates can be improved by enhancing the support of H263 provided by residue 262. The linear side chains of serine and alanine at this position provide more support than IMP-6's glycine, resulting in improved activity; however, valine's branched side chain is unfavorable. Thus, a fine balance between underpacking and overpacking appears to be required. The fact that all mutations at the more distant positions 121 and 218 had either no

effect (F218Y) or a negative effect (S121G and F218I) on the conversion of type II substrates suggests that this region is already highly optimized for these substrates. This is in agreement with a recent in vitro evolution study, which predicts that IMP-1 will not evolve to confer increased resistance to IMP (Hall 2004).

Support of H263 is not crucial for the hydrolysis of type I substrates (NIT, CEF, and CTX) because these substrates do not exert pressure on it. All investigated mutations that are indifferent or unfavorable for type II substrates have a beneficial effect on the conversion of type I substrates. In the absence of pressure on H263 and the region beyond it, these mutations probably stabilize the enzyme-substrate intermediate complex by improving packing or allowing more efficient zinc coordination geometry.

The strategy pursued very likely depends on which antibiotic imposes selective pressure. The evolution of IMP-6 to IMP-1 is probably the result of the application of IMP. Under the selective pressure of CEF or CTX, the mutants G262V, S121G, F218Y, and F218I might evolve. These antibiotics are already converted very efficiently by IMP-6 and IMP-1, but their inactivation can still be improved in vitro. Nevertheless, none of the investigated point mutants was superior to IMP-6 toward type I substrates or IMP-1 toward type II substrates when tested in vivo.

It is noteworthy that all point mutants selected for experimental validation based on molecular modeling (data not shown) had increased catalytic efficiencies toward at least one substrate compared to the wild type IMP-6 and in four cases even compared to the improved IMP-1. Positions 121 and 218 are strictly conserved in IMP-1 through IMP-13 (Docquier et al. 2003; Toleman et al. 2003), which might lead to the assumption that these enzymes do not tolerate or benefit from mutation at these positions. We have shown that such an assumption is incorrect. Materon and Palzkill have also found active IMP-1 mutants with mutations in conserved positions, including N233A, which was superior to IMP-1 in the conversion of AMP, NIT, CTX, and LOR (Materon and Palzkill 2001).

The same amino acids we tested in our mutants appear at structurally identical positions in other wild-type MBLs, indicating that these mutations are not deleterious and may be beneficial. Tyrosine is found at position 218 in the B1 enzyme VIM-1 (Lauretti et al. 1999), the B2 enzymes CphA (Massidda et al. 1991) and Sfh-I (Saavedra et al. 2003), and the B3 enzymes L1 (Walsh et al. 1994) and THIN-B (Rossolini et al. 2001). Isoleucine is found at the same position in the B3 enzymes FEZ-1 (Boschi et al. 2000) and GOB-1 (Bellais et al. 2000), and valine has been reported at position 262 in the B3 MBL THIN-B (Rossolini et al. 2001). Our mutants are all accessible by single nucleotide exchanges and all except F218I express and fold well. These findings indicate that there is tremendous evolutionary potential for MBLs to enhance catalytic efficiency. We propose that yet unidentified imipenemase variants carrying some of these mutations might exist and be isolated from patients in the future. This may be especially true for G262A and F218Y, which resulted in enzymes with good folding properties (Table 1), broad in vitro substrate spectra (Table 2 and Fig. 4) and the ability to confer high resistance levels in vivo (Table 3).

The lowest MICs were observed with CAZ and IMP (Table 3), indicating that their structural features, i.e. positively charged and non-electron-donor $R_2$ side chains, should be considered when designing novel β-lactam antibiotics.

**Materials and methods**

*Expression and purification*

The IMP-1 gene was cloned into the pET30a(+) plasmid in a way that the leader sequence was deleted, resulting in pIMP-1 for cytoplasmic expression of the enzyme under control of the T7 promoter (Hammond et al. 1999). This plasmid was kindly provided by Jeffrey H. Toney from the Merck Research Laboratories (Rahway, NJ). IMP-6 and variant genes were constructed from IMP-1 using PCR-based site-directed mutagenesis. Proteins were expressed by IPTG induction (0.5 mM final concentration) in *Escherichia coli* BL21(DE3) hosts (Stratagene) at 22 °C. Cells were lysed by sonification in 50 mM 4-morpholinepropanesulfonic acid (MOPS) buffer, pH 7.0, containing 100 μM zinc sulfate. Soluble and insoluble fractions were separated by centrifugation at 20,000 g for 30 min and analyzed by sodium dodecyl sulfate-polyacrylamide gel electrophoresis (SDS-PAGE). The relative amounts of enzyme expressed were estimated from SDS-PAGE. The percentages of soluble enzyme (Table 1) were estimated by comparing the intensity of the ~25 kDa band in the soluble fraction with the corresponding band in the insoluble fraction after applying equivalent volumes to SDS-PAGE. Mutants G262A and F218Y had the highest yield of soluble protein (50%) and F218I had the lowest yield (2%). MBLs in the soluble fractions were purified to homogeneity by ion exchange chromatography using a salt gradient from 0 to 500 mM sodium chloride and gel filtration. Per one liter of culture, between 20 and 100 ml of purified protein solution was recovered. Protein masses were verified by electrospray ionization mass spectrometry, and protein concentrations were determined in triplet using the Bio-Rad Protein Assay kit with BSA as standard (Table I). Mutant G262A was expressed, purified, and its protein concentration was measured twice. Thus, the protein concentration of G262A shown in Table 1 represents the average ± the standard deviation of six measurements (two sets of triplicates).

*Biophysical Characterization*

Circular dichroism spectra were collected after dialysis of the purified enzymes against zinc-free 50 mM sodium phosphate buffer, pH 7.0. Depending on the protein concentration, 3 to 10 scans from 250 to 190 nm were averaged. The zinc content of the MBLs was determined using the 4-(2-pyridylazo)resorcinol (PAR) assay as reported (Fast et al. 2001), except that MOPS buffer was used instead of HEPES buffer. Protein concentrations in the dialyzed samples were determined using the Bio-Rad Protein Assay kit with BSA as standard. Both preparations of G262A were assayed.

*Kinetic constants*

To protect enzymes from denaturation, 100 μg/ml BSA was added to purified proteins directly after gel filtration. Kinetic constants were obtained for the following substrates: PEN, AMP, CEF, CTX (Sigma), NIT (Oxoid), CAZ (Glaxo Smith Kline), and IMP (Merck). Enzymes were diluted in MOPS buffer, pH 7.0, containing 100 μM zinc sulfate and 10 μg/ml BSA and preincubated at 30 °C. Substrate was added at different concentrations and initial velocities were determined by measuring formation of product (for NIT) (Wang et al. 1999) or degradation of substrate (for all other substrates) (Laraki et al. 1999) at 30 °C, using the published wavelengths and extinction coefficients. Three series of measurements were carried out for each enzyme preparation (two preparations for G262A and one for all other enzymes). $k_{cat}$ and $K_M$ values were calculated by fitting the data to the Michaelis Menten equation or to a modified version that accounts for substrate inhibition (Simm et al. 2001) for each series. $k_{cat}/K_M$ values were determined independently for each series and the data shown in Table 2 and Figs. 3 and 4 represent the averages and standard deviations of these values. When substrate inhibition was observed, catalytic efficiencies were calculated using the apparent productive substrate binding constant $K_{app}$ rather than $K_M$. Also $K_{app}$ and the inhibition constant $K_i$ were determined independently for each series and averages ± standard deviations are presented in Table 2.

*Susceptibility assay*

MICs were determined by adding β-lactam antibiotics at different concentrations to 1:20 dilutions of over-night cultures of *E. coli* BL21(DE3) cells harboring the plasmids for expression of MBLs in LB medium containing 30 μg/ml kanamycin (Hammond et al. 1999). This assay was carried out in a 96-well-plate format without IPTG induction, thus taking advantage of the not very tightly regulated T7 promoter. MICs were defined as the lowest antibiotic concentration that inhibited growth visible under a stereomicroscope with 25-fold magnification. *E. coli* BL21(DE3) transformed with the plasmid pNEG served as a negative control. pNEG is a derivative of pIMP-1, of which the major part of the IMP-1 gene was excised using *Hind*III.

**Acknowledgments**

We thank Jeffrey H. Toney (formerly with Merck) for providing a plasmid containing the IMP-1 gene, Merck for the gift of imipenem, and Marie Ary for assistance with the manuscript. This work was supported by the Colvin Biology Fellowship at Caltech (to P.O.), the Howard Hughes Medical Institute, the Ralph M. Parsons Foundation, and an IBM Shared University research grant (to S.L.M.).

**References**

Ambler, R. 1980. The structure of β-lactamases. *Philos Trans Roy Soc Lond B Biol Sci* **289:** 321-331.

Antony, J., Gresh, N., Olsen, L., Hemmingsen, L., Schofield, C.J., and Bauer, R. 2002. Binding of D- and L-captopril inhibitors to metallo-β-lactamase studied by polarizable molecular mechanics and quantum mechanics. *J Comput Chem* **23:** 1281-1296.

Bellais, S., Aubert, D., Naas, T., and Nordmann, P. 2000. Molecular and biochemical heterogeneity of class B carbapenem-hydrolyzing β-lactamases in Chryseobacterium meningosepticum. *Antimicrob Agents Chemother* **44:** 1878-1886.

Boschi, L., Mercuri, P.S., Riccio, M.L., Amicosante, G., Galleni, M., Frere, J.M., and Rossolini, G.M. 2000. The Legionella (Fluoribacter) gormanii metallo-b-lactamase: a new member of the highly divergent lineage of molecular-subclass B3 β-lactamases. *Antimicrob Agents Chemother* **44:** 1538-1543.

Carenbauer, A.L., Garrity, J.D., Periyannan, G., Yates, R.B., and Crowder, M.W. 2002. Probing substrate binding to metallo-β-lactamase L1 from Stenotrophomonas maltophilia by using site-directed mutagenesis. *BMC Biochem* **3:** 4.

Carfi, A., Pares, S., Duee, E., Galleni, M., Duez, C., Frere, J.M., and Dideberg, O. 1995. The 3-D structure of a zinc metallo-β-lactamase from

Bacillus cereus reveals a new type of protein fold. *Embo J* **14:** 4914-4921.

Concha, N.O., Janson, C.A., Rowling, P., Pearson, S., Cheever, C.A., Clarke, B.P., Lewis, C., Galleni, M., Frere, J.M., Payne, D.J., et al. 2000. Crystal structure of the IMP-1 metallo β-lactamase from Pseudomonas aeruginosa and its complex with a mercaptocarboxylate inhibitor: binding determinants of a potent, broad-spectrum inhibitor. *Biochemistry* **39:** 4288-4298.

Concha, N.O., Rasmussen, B.A., Bush, K., and Herzberg, O. 1996. Crystal structure of the wide-spectrum binuclear zinc β-lactamase from Bacteroides fragilis. *Structure* **4:** 823-836.

de Seny, D., Prosperi-Meys, C., Bebrone, C., Rossolini, G.M., Page, M.I., Noel, P., Frere, J.M., and Galleni, M. 2002. Mutational analysis of the two zinc-binding sites of the Bacillus cereus 569/H/9 metallo-β-lactamase. *Biochem J* **363:** 687-696.

Docquier, J.D., Riccio, M.L., Mugnaioli, C., Luzzaro, F., Endimiani, A., Toniolo, A., Amicosante, G., and Rossolini, G.M. 2003. IMP-12, a New Plasmid-Encoded Metallo-β-Lactamase from a Pseudomonas putida Clinical Isolate. *Antimicrob Agents Chemother* **47:** 1522-1528.

Fast, W., Wang, Z., and Benkovic, S.J. 2001. Familial mutations and zinc stoichiometry determine the rate-limiting step of nitrocefin hydrolysis by metallo-β-lactamase from Bacteroides fragilis. *Biochemistry* **40:** 1640-1650.

Franceschini, N., Caravelli, B., Docquier, J.D., Galleni, M., Frere, J.M., Amicosante, G., and Rossolini, G.M. 2000. Purification and biochemical characterization of the VIM-1 metallo-β-lactamase. *Antimicrob Agents Chemother* **44:** 3003-3007.

Galleni, M., Lamotte-Brasseur, J., Rossolini, G.M., Spencer, J., Dideberg, O., and Frere, J.M. 2001. Standard numbering scheme for class B β-lactamases. *Antimicrob Agents Chemother* **45:** 660-663.

Garcia-Saez, I., Mercuri, P.S., Papamicael, C., Kahn, R., Frere, J.M., Galleni, M., Rossolini, G.M., and Dideberg, O. 2003. Three-dimensional structure of FEZ-1, a monomeric subclass B3 metallo-β-lactamase from Fluoribacter gormanii, in native form and in complex with D-captopril. *J Mol Biol* **325:** 651-660.

Hall, B.G. 2004. In vitro evolution predicts that the IMP-1 metallo-β-lactamase does not have the potential to evolve increased activity against imipenem. *Antimicrob Agents Chemother* **48:** 1032-1033.

Hammond, G.G., Huber, J.L., Greenlee, M.L., Laub, J.B., Young, K., Silver, L.L., Balkovec, J.M., Pryor, K.D., Wu, J.K., Leiting, B., et al. 1999. Inhibition of IMP-1 metallo-β-lactamase and sensitization of IMP-1-producing bacteria by thioester derivatives. *FEMS Microbiol Lett* **179:** 289-296.

Haruta, S., Yamaguchi, H., Yamamoto, E.T., Eriguchi, Y., Nukaga, M., O'Hara, K., and Sawai, T. 2000. Functional analysis of the active site of a metallo-β-lactamase proliferating in Japan. *Antimicrob Agents Chemother* **44:** 2304-2309.

Haruta, S., Yamamoto, E.T., Eriguchi, Y., and Sawai, T. 2001. Characterization of the active-site residues asparagine 167 and lysine 161 of the IMP-1 metallo β-lactamase. *FEMS Microbiol Lett* **197:** 85-89.

Hayes, R.J., Bentzien, J., Ary, M.L., Hwang, M.Y., Jacinto, J.M., Vielmetter, J., Kundu, A., and Dahiyat, B.I. 2002. Combining computational and experimental screening for rapid optimization of protein properties. *Proc Natl Acad Sci U S A* **99:** 15926-15931.

Huntley, J.J., Fast, W., Benkovic, S.J., Wright, P.E., and Dyson, H.J. 2003. Role of a solvent-exposed tryptophan in the recognition and binding of antibiotic substrates for a metallo-β-lactamase. *Protein Sci* **12:** 1368-1375.

Huntley, J.J., Scrofani, S.D., Osborne, M.J., Wright, P.E., and Dyson, H.J. 2000. Dynamics of the metallo-β-lactamase from Bacteroides fragilis in

the presence and absence of a tight-binding inhibitor. *Biochemistry* **39:** 13356-13364.

Iyobe, S., Kusadokoro, H., Ozaki, J., Matsumura, N., Minami, S., Haruta, S., Sawai, T., and O'Hara, K. 2000. Amino acid substitutions in a variant of IMP-1 metallo-β-lactamase. *Antimicrob Agents Chemother* **44:** 2023-2027.

Laraki, N., Franceschini, N., Rossolini, G.M., Santucci, P., Meunier, C., de Pauw, E., Amicosante, G., Frere, J.M., and Galleni, M. 1999. Biochemical characterization of the Pseudomonas aeruginosa 101/1477 metallo-β-lactamase IMP-1 produced by Escherichia coli. *Antimicrob Agents Chemother* **43:** 902-906.

Lauretti, L., Riccio, M.L., Mazzariol, A., Cornaglia, G., Amicosante, G., Fontana, R., and Rossolini, G.M. 1999. Cloning and characterization of blaVIM, a new integron-borne metallo-β-lactamase gene from a Pseudomonas aeruginosa clinical isolate. *Antimicrob Agents Chemother* **43:** 1584-1590.

Livermore, D.M., and Woodford, N. 2000. Carbapenemases: a problem in waiting? *Curr Opin Microbiol* **3:** 489-495.

Massidda, O., Rossolini, G.M., and Satta, G. 1991. The Aeromonas hydrophila cphA gene: molecular heterogeneity among class B metallo-β-lactamases. *J Bacteriol* **173:** 4611-4617.

Materon, I.C., and Palzkill, T. 2001. Identification of residues critical for metallo-β-lactamase function by codon randomization and selection. *Protein Sci* **10:** 2556-2565.

Moali, C., Anne, C., Lamotte-Brasseur, J., Groslambert, S., Devreese, B., Van Beeumen, J., Galleni, M., and Frere, J.M. 2003. Analysis of the Importance of the Metallo-β-Lactamase Active Site Loop in Substrate Binding and Catalysis. *Chem Biol* **10:** 319-329.

Oelschlaeger, P., Schmid, R.D., and Pleiss, J. 2003a. Insight into the mechanism of the IMP-1 metallo-β-lactamase by molecular dynamics simulations. *Protein Eng* **16:** 341-350.

Oelschlaeger, P., Schmid, R.D., and Pleiss, J. 2003b. Modeling domino effects in enzymes: Molecular basis of the substrate specificity of the

bacterial metallo-β-lactamases IMP-1 and IMP-6. *Biochemistry* **42:** 8945-8956.

Orencia, M.C., Yoon, J.S., Ness, J.E., Stemmer, W.P., and Stevens, R.C. 2001. Predicting the emergence of antibiotic resistance by directed evolution and structural analysis. *Nat Struct Biol* **8:** 238-242.

Ponsard, I., Galleni, M., Soumillion, P., and Fastrez, J. 2001. Selection of metalloenzymes by catalytic activity using phage display and catalytic elution. *Chembiochem* **2:** 253-259.

Rossolini, G.M., Condemi, M.A., Pantanella, F., Docquier, J.D., Amicosante, G., and Thaller, M.C. 2001. Metallo-β-lactamase producers in environmental microbiota: new molecular class B enzyme in Janthinobacterium lividum. *Antimicrob Agents Chemother* **45:** 837-844.

Saavedra, M.J., Peixe, L., Sousa, J.C., Henriques, I., Alves, A., and Correia, A. 2003. Sfh-I, a subclass B2 metallo-β-lactamase from a Serratia fonticola environmental isolate. *Antimicrob Agents Chemother* **47:** 2330-2333.

Salsbury, F.R., Jr., Crowley, M.F., and Brooks, C.L., 3rd. 2001. Modeling of the metallo-β-lactamase from B. fragilis: structural and dynamic effects of inhibitor binding. *Proteins* **44:** 448-459.

Scrofani, S.D., Chung, J., Huntley, J.J., Benkovic, S.J., Wright, P.E., and Dyson, H.J. 1999. NMR characterization of the metallo-β-lactamase from Bacteroides fragilis and its interaction with a tight-binding inhibitor: role of an active-site loop. *Biochemistry* **38:** 14507-14514.

Siemann, S., Evanoff, D.P., Marrone, L., Clarke, A.J., Viswanatha, T., and Dmitrienko, G.I. 2002. N-arylsulfonyl hydrazones as inhibitors of IMP-1 metallo-β-lactamase. *Antimicrob Agents Chemother* **46:** 2450-2457.

Simm, A.M., Higgins, C.S., Pullan, S.T., Avison, M.B., Niumsup, P., Erdozain, O., Bennett, P.M., and Walsh, T.R. 2001. A novel metallo-β-lactamase, Mbl1b, produced by the environmental bacterium Caulobacter crescentus. *FEBS Lett* **509:** 350-354.

Suarez, D., Brothers, E.N., and Merz, K.M., Jr. 2002a. Insights into the Structure and Dynamics of the Dinuclear Zinc β-Lactamase Site from Bacteroides fragilis. *Biochemistry* **41:** 6615-6630.

Suarez, D., Diaz, N., and Merz, K.M., Jr. 2002b. Molecular dynamics simulations of the dinuclear zinc-β-lactamase from Bacteroides fragilis complexed with imipenem. *J Comput Chem* **23:** 1587-1600.

Toleman, M.A., Biedenbach, D., Bennett, D., Jones, R.N., and Walsh, T.R. 2003. Genetic characterization of a novel metallo-β-lactamase gene, blaIMP13, harboured by a novel Tn5051-type transposon disseminating carbapenemase genes in Europe: report from the SENTRY worldwide antimicrobial surveillance programme. *J Antimicrob Chemother*.

Voigt, C.A., Martinez, C., Wang, Z.G., Mayo, S.L., and Arnold, F.H. 2002. Protein building blocks preserved by recombination. *Nat Struct Biol* **9:** 553-558.

Walsh, T.R., Hall, L., Assinder, S.J., Nichols, W.W., Cartwright, S.J., MacGowan, A.P., and Bennett, P.M. 1994. Sequence analysis of the L1 metallo-β-lactamase from Xanthomonas maltophilia. *Biochim Biophys Acta* **1218:** 199-201.

Wang, Z., Fast, W., and Benkovic, S.J. 1999. On the mechanism of the metallo-β-lactamase from Bacteroides fragilis. *Biochemistry* **38:** 10013-10023.

Yanchak, M.P., Taylor, R.A., and Crowder, M.W. 2000. Mutational analysis of metallo-β-lactamase CcrA from Bacteroides fragilis. *Biochemistry* **39:** 11330-11339.

Yang, Y., Keeney, D., Tang, X., Canfield, N., and Rasmussen, B.A. 1999. Kinetic properties and metal content of the metallo-β-lactamase CcrA harboring selective amino acid substitutions. *J Biol Chem* **274:** 15706-15711.

**Table 1.** *Biophysical characteristics of the purified proteins*

| MBL | % soluble | Concentration after purification (μM)[a] | Molecular mass (calculated) | Zinc ions / molecule[b] |
|---|---|---|---|---|
| IMP-6 | 30 | 16.7 ± 0.3 | 25081.2 (25082.7) | 1.9 ± 0.2 |
| IMP-1 (G262S) | 20 | 9.2 ± 0.4 | 25112.2 (25112.7) | 2.0 ± 0.2 |
| G262A | 50 | 7.4 ± 1.1 | 25096.3 (25096.7) | 2.0 ± 0.4 |
| G262V | 10 | 4.3 ± 0.2 | 25124.8 (25124.8) | 2.2 ± 0.1 |
| S121G | 15 | 3.3 ± 0.2 | 25054.7 (25052.7) | 2.9 ± 0.2 |
| F218Y | 50 | 14.0 ± 0.7 | 25098.2 (25098.7) | 2.1 ± 0.3 |
| F218I | 2 | 0.15 ± 0.01 | 25047.6 (25048.7) | |

[a] Values are average ± standard deviation of at least three measurements.

[b] Values are average ± deviation of at least two independent experiments.

**Table 2.** *Kinetic constants of wild types IMP-1 and IMP-6 and five mutants with seven β-lactam antibiotics*

| Enzyme | Kinetic constant | Antibiotic | | | | | | |
|---|---|---|---|---|---|---|---|---|
| | | NIT | CEF | CTX | CAZ | PEN | AMP | IMP |
| IMP-6 | $k_{cat}$ ($s^{-1}$) | 277± 14 | 147 ±32 | 26.4 ±2.1 | 4.4 ±0.5 | 401 ±46 | 158 ±11 | 96 ±15 |
| | | | *384 ±11*[a] | *54.8 ±5.3*[a] | *3.6 ±0.2*[a] | *21.6 ±1.0*[a] | *11.8 ±1.4*[a] | *132 ±8*[a] |
| | $K_M$ (μM) | 10.0 ±1.6 | 14.7 ±4.1 | 9.0 ±1.3 | 54 ±9 | 998 ±125 | 406 ±40 | 68 ±19 |
| | | | *9.8 ±0.3*[a] | *3.0± 0.3*[a] | *118 ±19*[a] | *464 ±60*[a] | *437 ±105*[a] | *1280 ±120*[a] |
| | $k_{cat}/K_M$ ($s^{-1}$ $μM^{-1}$) | 28.0 ±3.3 | 10.1 ±0.8 | 2.9 ±0.2 | 0.082 ±0.005 | 0.40 ±0.01 | 0.39 ±0.01 | 1.43 ±0.19 |
| | | | *39.2*[a] | *18.3*[a] | *0.031*[a] | *0.047*[a] | *0.027*[a] | *0.10*[a] |
| IMP-1 (G262S) | $k_{cat}$ ($s^{-1}$) | 229 ±11 | 64.5 ±5.7 | 19.0 ±4.1 | 12.2 ±2.0 | 713 ±3 | 154 ±18 | 77 ±4 |
| | | *228 ±11*[b] *260 ±22*[c] | *65.0 ±2.9*[a] | *22.5 ±1.4*[a] | *16.3 ±0.9*[a] | *461 ±17*[a] | *162 ±15*[a] | *127 ±11*[a] |
| | $K_M$ (μM) | 9.7 ±0.8 | 7.4 ±1.3 | 6.9 ±3.1 | 44 ±13 | 445 ±16 | 223 ±44 | 25 ±2 |
| | | *9 ±3*[b] *12 ±1*[c] | *2.0 ±0.1*[a] | *1.4 ±0.1*[a] | *46.0 ±1.4*[a] | *241 ±10*[a] | *140 ±9*[a] | *30.0 ±3.9*[a] |
| | $k_{cat}/K_M$ ($s^{-1}$ $μM^{-1}$) | 23.8 ±1.0 | 8.8 ±0.7 | 2.9 ±0.6 | 0.28 ±0.04 | 1.60 ±0.06 | 0.70 ±0.07 | 3.1 ±0.1 |
| | | *25.3*[b] *21.7*[c] | *32.5*[a] | *16.1*[a] | *0.35*[a] | *1.9*[a] | *1.2*[a] | *4.2*[a] |

| | | | | | | | | |
|---|---|---|---|---|---|---|---|---|
| G262A | $k_{cat}$ ($s^{-1}$) | 233 | 45.7 | 24.4 | 19.7 | 1060 | 80 | 43.8 |
| | | ±11 | ±1.0 | ±2.6 | ±2.7 | ±130 | ±9 | ±2.7 |
| | $K_M$ (μM) | 10.7 | 5.2 | 7.6 | 95 | 1230 | 157 | 22.7 |
| | | ±1.8 | ±0.5 | ±1.1 | ±17 | ±190 | ±26 | ±3.1 |
| | $k_{cat}/K_M$ | 22.2 | 8.9 | 3.2 | 0.21 | 0.87 | 0.52 | 1.95 |
| | ($s^{-1}$ $\mu M^{-1}$) | ±2.8 | ±0.8 | ±0.2 | ±0.01 | ±0.05 | ±0.08 | ±0.17 |
| G262V | $k_{cat}$ ($s^{-1}$) | 459 | 247 | 99 | 0.4 | 17 | 10.6 | 5.8 |
| | | ±23 | ±11 | ±14 | ±0.1 | ±5 | ±1.6 | ±2.2 |
| | $K_M$ (μM) | 4.6 | 16.8 | 17 | 61 | 1200 | 1350 | 124 |
| | | ±1.0 | ±1.8 | ±6 | ±4 | ±320 | ±240 | ±51 |
| | $k_{cat}/K_M$ | 102 | 14.7 | 6.1± | 0.007 | 0.014 | 0.0079 | 0.047 |
| | ($s^{-1}$ $\mu M^{-1}$) | ±18 | ±1.0 | 1.1 | ±0.002 | ±0.001 | ±0.0003 | ±0.001 |
| S121G | $k_{cat}$ ($s^{-1}$) | 779 | 503 | 77 | 5.2 | 95 | 24.6 | 76 |
| | | ±162 | ±35 | ±7 | ±1.8 | ±20 | ±2.3 | ±24 |
| | $K_M$ [$K_{app}$] | 11.3 | 30.2 | 8.0 | 123 | 504 | 260 | 250 |
| | (μM) | ±3.1 | ±4.8 | ±1.3 | ±50 | ±134 | ±52 | ±91 |
| | $K_i$ (μM) | 54± 16 | | | | | | |
| | $k_{cat}/K_M$ | 69.5 | 16.8 | 9.6 | 0.043 | 0.19 | 0.096 | 0.31 |
| | [$k_{cat}/K_{app}$] | ±4.7 | ±1.6 | ±0.8 | ±0.004 | ±0.02 | ±0.012 | ±0.02 |
| | ($s^{-1}$ $\mu M^{-1}$) | | | | | | | |
| F218Y | $k_{cat}$ ($s^{-1}$) | 446 | 178 | 33.4 | 5.3 | 237 | 129 | 82 |
| | | ±44 | ±1 | ±1.4 | ±0.5 | ±15 | ±13 | ±22 |
| | $K_M$ [$K_{app}$] | 7.4 | 8.1 | 4.7 | 62 | 545 | 272 | 66 |
| | (μM) | ±1.5 | ±0.5 | ±1.1 | ±5 | ±51 | ±42 | ±27 |
| | $K_i$ (μM) | 146 | | | | | | |
| | | ±32 | | | | | | |
| | $k_{cat}/K_M$ | 61.4 | 21.9 | 7.3 | 0.085 | 0.44 | 0.48 | 1.3 |
| | [$k_{cat}/K_{app}$] | ±5.9 | ±1.2 | ±1.5 | ±0.001 | ±0.02 | ±0.03 | ±0.2 |
| | ($s^{-1}$ $\mu M^{-1}$) | | | | | | | |

| | | | | | | | | |
|---|---|---|---|---|---|---|---|---|
| F218I | $k_{cat}$ ($s^{-1}$) | 1385 | 655 | 93 | 6.6 | 129 | 82 | 130 |
| | | ±16 | ±21 | ±5 | ±0.5 | ±23 | ±7 | ±20 |
| | $K_M$ (μM) | 5.9 | 14.6 | 5.1 | 101 | 608 | 543 | 219 |
| | | ±0.1 | ±1.3 | ±0.8 | ±7 | ±160 | ±60 | ±23 |
| | $k_{cat}/K_M$ | 235 | 45.0 | 18.3 | 0.065 | 0.22 | 0.15 | 0.59 |
| | ($s^{-1}$ $\mu M^{-1}$) | ±3 | ±2.6 | ±2.2 | ±0.001 | ±0.03 | ±0.01 | ±0.03 |

$K_i$ is the inhibition constant and $K_{app}$ the apparent productive substrate binding constant obtained from a Michaelis Menten fit that accounts for substrate inhibition (Simm et al. 2001). Values for this study are the means ± standard deviations of at least three determinations.

[a] Values reported by Iyobe et al. (Iyobe et al. 2000)

[b] Values reported by Materon and Palzkill (Materon and Palzkill 2001).

[c] Values reported by Siemann et al. (Siemann et al. 2002).

**Table 3.** *Resistance levels conferred by the wild-type and mutant enzymes*

| | MIC (μg/ml) of antibiotic | | | | | |
|---|---|---|---|---|---|---|
| Enzyme | CEF | CTX | CAZ | PEN | AMP | IMP |
| (-)[a] | 16 | 8 | 64 | 64 | 8 | 2 |
| IMP-6 | 2048 | 1024 | 128 | 1024 | 128 | 256 |
| IMP-1 | 1024 | 1024 | 256 | 4096 | 1024 | >1024 |
| G262A | 1024 | 1024 | 128 | 4096 | 512 | 512 |
| G262V | 128 | 32 | 32 | 64 | 8 | 4 |
| S121G | 1024 | 512 | 64 | 512 | 128 | 64 |
| F218Y | 2048 | 1024 | 64 | 1024 | 256 | 64 |
| F218I | 256 | 128 | 64 | 64 | 16 | 8 |

[a] (-), negative control: no expression of MBL.

**Figure legends**

**Figure 1.** Stereo view of a molecular model of the active site of IMP-1 bound to substrate CAZ. CAZ is shown in balls and sticks, zinc ions are shown as cyan spheres, zinc ligating amino acids appear as blue sticks, and the residues mutated in this study are shown as orange sticks.

**Figure 2.** Structures of the investigated β-lactam substrates. Type I substrates (NIT, CEF, and CTX) have $R_2$ side chains (boxed) that contain electron donors, while type II substrates have axial methyl groups (PEN and AMP) or positively charged $R_2$ side chains (CAZ and IMP).

**Figure 3.** Catalytic efficiencies ($k_{cat}/K_M$) of wild type enzymes IMP-6 and IMP-1 toward seven β-lactam antibiotics: NIT (*A*), other substrates (*B*). Error bars show standard deviation for at least three measurements. Substrate profiles are similar to those reported previously.
a) Materon and Palzkill (Materon and Palzkill 2001),
b) Siemann et al. (Siemann et al. 2002), and
c) Iyobe et al. (Iyobe et al. 2000).

**Figure 4.** Catalytic efficiencies ($k_{cat}/K_M$) of mutants compared to wild type enzymes IMP-6 and IMP-1 toward seven β-lactam antibiotics. Error bars show standard deviation for at least three measurements. Type I substrates (top) are hydrolyzed much more efficiently and show a different profile from type II substrates (bottom).

**Figure 1.** Oelschlaeger et al.

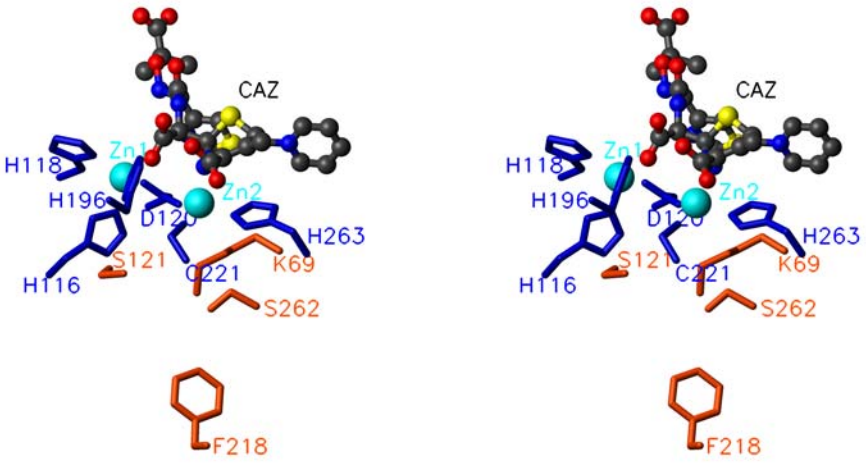

**Figure 2.** Oelschlaeger et al.

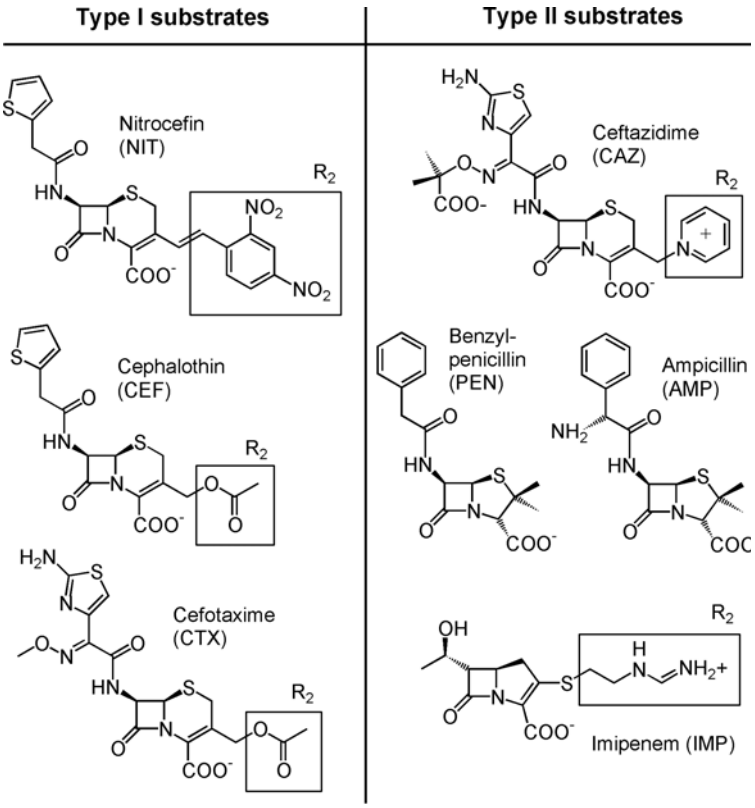

**Figure 3.** Oelschlaeger et al.

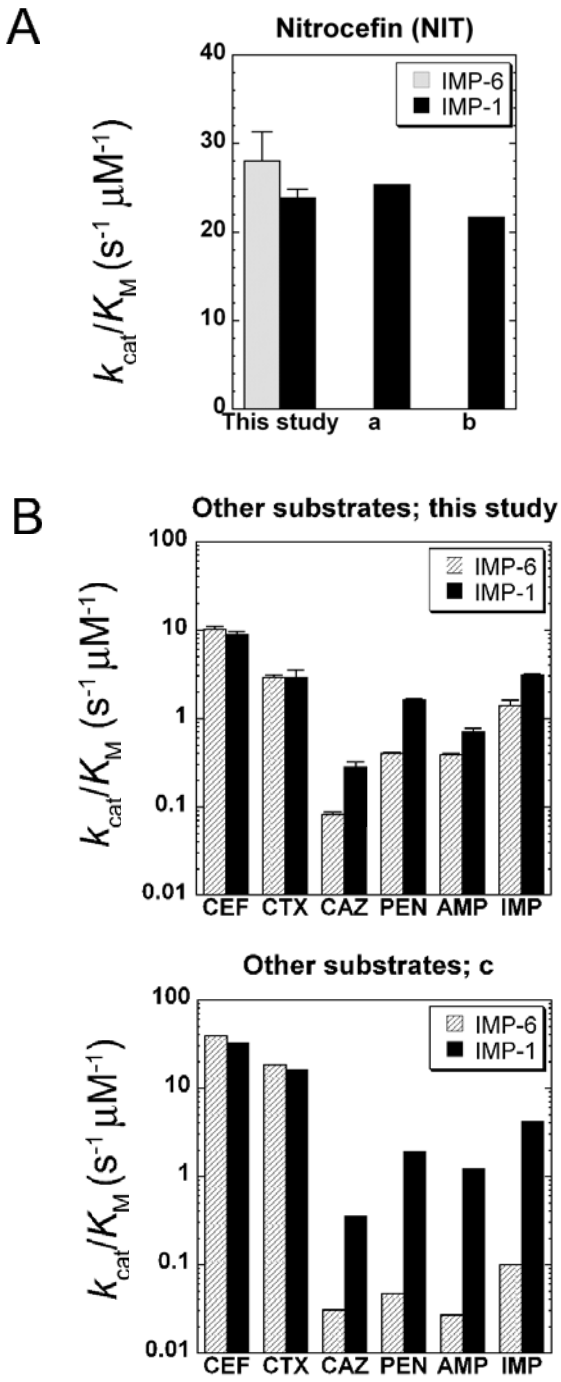

**Figure 4.** Oelschlaeger et al.